Detecting the $L_\mu - L_\tau$ gauge boson at Belle II

Takeshi Araki,[1,*] Shihori Hoshino,[1,†] Toshihiko Ota,[1,2,‡] Joe Sato,[1,§] and Takashi Shimomura[3,‖]

[1]*Department of Physics, Saitama University, Shimo-Okubo 255, 338-8570 Saitama Sakura-ku, Japan*
[2]*Department of Physics, Yachay Tech, Hacienda San José s/n y Proyecto Yachay,*
100119 San Miguel de Urcuquí, Ecuador
[3]*Faculty of Education, University of Miyazaki, 1-1 Gakuen-Kibanadai-Nishi, 889-2192 Miyazaki, Japan*

We discuss the feasibility of detecting the gauge boson of the $U(1)_{L_\mu - L_\tau}$ symmetry, which possesses a mass in the range between MeV and GeV, at the Belle-II experiment. The kinetic mixing between the new gauge boson Z' and photon is forbidden at the tree level and is radiatively induced. The leptonic force mediated by such a light boson is motivated by the discrepancy in muon anomalous magnetic moment and also the gap in the energy spectrum of cosmic neutrino. Defining the process $e^+ e^- \to \gamma Z' \to \gamma \nu \bar{\nu}$ (*missing energy*) to be the signal, we estimate the numbers of the signal and the background events and show the parameter region to which the Belle-II experiment will be sensitive. The signal process in the $L_\mu - L_\tau$ model is enhanced with a light Z', which is a characteristic feature differing from the dark photon models with a constant kinetic mixing. We find that the Belle-II experiment with the design luminosity will be sensitive to the Z' with the mass $M_{Z'} \lesssim 1$ GeV and the new gauge coupling $g_{Z'} \gtrsim 8 \times 10^{-4}$, which covers a half of the unconstrained parameter region that explains the discrepancy in muon anomalous magnetic moment. The possibilities to improve the significance of the detection are also discussed.

I. INTRODUCTION

The experimental confirmation of the standard model (SM) of particle physics was completed by the discovery of the Higgs boson at the Large Hadron Collider (LHC) in 2012 [1,2]. Although the SM successfully describes most of phenomena in nature below the electroweak scale, well-established observations such as nonzero masses of neutrinos [3,4], the existence of dark matter (DM) [5] and dark energy [6,7], and the matter-antimatter asymmetry in the Universe, strongly require extensions of the SM. Despite continuous and intense effort to search for new physics at the high-energy frontier currently pushed by the LHC Run II, any clear sign of it has not been obtained yet. Therefore, many attempts to discover a faint hint of new physics have been made and are also newly planed in the low-energy region. In fact, extensions of the SM with a new boson possessing a mass around the MeV scale and only feebly interacting with our visible sector have been recently discussed in much literature, which is motivated by phenomenological observations. Those include the discrepancy between the SM predictions and the experimental measurements of the muon anomalous magnetic moment [8,9], inconsistency in the measurement of the $e^+ e^-$ pair produced in the transition between an excited state of ^{8}Be

and its ground state [10–15], the tension between the sterile neutrino suggested by the short-baseline neutrino experiments and cosmological observations [16–18], the deficit of high-energy cosmic neutrino events, which is reported by the IceCube experiment [19–27], and the disagreement in the measurement of the proton radius [28–31]. It is also known that a light force carrier that intermediates between the DM promotes the annihilation of the DM in the early Universe and helps to reproduce the correct relic density [32,33]. As a theoretical framework of such a light boson, the gauged $U(1)_{L_\mu - L_\tau}$ model [34–36] has particularly gained a lot of attention, because the model is free from gauge anomaly without any extension of particle content. Moreover, recent studies reveal that the gauge boson with an MeV-scale mass, which resolves the discrepancy in muon anomalous magnetic moment, can simultaneously explain either the deficit in the high-energy cosmic neutrino spectrum [23–26] or the problem of the relic abundance of DM in the scenario with a light weakly interacting massive particle [37–40]. The $L_\mu - L_\tau$ symmetry has been discussed also in the context of the lepton-flavor nonuniversality in B decays [41–43], lepton-flavor-violating decay of the Higgs boson [42,44], the flavor structure of neutrino mass matrix [40,45–49], and dark matter phenomenology [38,40,43,49].[1]

In this paper, we propose a test of the models with the $U(1)_{L_\mu - L_\tau}$ gauge symmetry which is spontaneously broken

*araki@krishna.th.phy.saitama-u.ac.jp
†hoshino@krishna.th.phy.saitama-u.ac.jp
‡tota@yachaytech.edu.ec
§joe@phy.saitama-u.ac.jp
‖shimomura@cc.miyazaki-u.ac.jp

[1]For phenomenology of light extra $U(1)$ gauge bosons in general, see e.g., Refs. [50–64].

below the electroweak scale, by searching for the process $e^+e^- \to \gamma + missing\,energy$ at the upcoming Belle-II experiment. Among the decay channels of Z', we focus on $Z' \to \nu\bar{\nu}$ as the signal channel, because the signal is imitated only by the weak interaction processes and does not suffer from electromagnetic background, as long as the final state particles are not missed at the detector. Since the cross section of the signal event is inversely proportional to the square of the center-of-mass energy, the colliders with a low energy are expected to be suitable for this type of search. The high luminosity of the Belle-II experiment also conduces to a good sensitivity to a feeble interaction. The sensitivity of the B-factories to a new light gauge boson, which is often called the dark photon,[2] has been studied in the literature [65–68] with the assumption that the kinetic mixing between the electromagnetic $U(1)_{\mathrm{em}}$ and the $U(1)$ for the dark photon is given as a constant parameter. In contrast, it is not introduced as a free parameter in the minimal $U(1)_{L_\mu-L_\tau}$ model dealt in this paper. In the minimal $U(1)_{L_\mu-L_\tau}$ model, only two parameters are newly introduced, which are the new gauge coupling constant and the mass of the Z'. As a consequence, the kinetic mixing arises radiatively, and hence it is not a constant but depends on the new gauge coupling and the momentum carried by the photon and the Z'. We see in the next section that the signal event in the minimal $U(1)_{L_\mu-L_\tau}$ model is enhanced with the light $M_{Z'}$ with which the discrepancy in muon anomalous magnetic moment and the deficit in the cosmic neutrino spectrum can be simultaneously explained. There is no such enhancement mechanism in the models with a constant kinetic mixing.

This paper is organized as follows. In the next section, we illustrate the minimal $U(1)_{L_\mu-L_\tau}$ model and list the constraints to the model parameters from various experiments. The motivations for the leptonic force mediated with such a new light gauge boson are discussed in Sec. II C. In Sec. III, we estimate the numbers of the signal and the background events and study the feasibility of detecting the Z' at the Belle-II experiment quantitatively. The ways to improve the sensitively are also discussed in Sec. III C. Finally, we mention another type of background in Sec. III D and draw conclusions in Sec. IV.

II. THE MINIMAL $L_\mu - L_\tau$ MODEL

Here we describe our model and list the experimental constraints to the relevant parameter space.

A. Lagrangian

We extend the SM with a new $U(1)$ gauge symmetry associated with the muon number minus the tau number,

i.e., $U(1)_{L_\mu-L_\tau}$, which leads to the following new leptonic gauge interactions:

$$\mathcal{L}_{\mathrm{int}} = g_{Z'}Q_{\alpha\beta}(\bar{\ell}_\alpha\gamma^\rho\ell_\beta + \bar{\nu}_\alpha\gamma^\rho P_L\nu_\beta)Z'_\rho, \qquad (1)$$

where Z' is the $U(1)_{L_\mu-L_\tau}$ gauge boson, ℓ_α and ν_α are charged leptons and neutrinos with flavor $\alpha = \{e,\mu,\tau\}$, $g_{Z'}$ is the gauge coupling constant of $U(1)_{L_\mu-L_\tau}$, and the diagonal matrix $Q_{\alpha\beta} = \mathrm{diag}(0,1,-1)$ gives the $U(1)_{L_\mu-L_\tau}$ charges. We assume that the $U(1)_{L_\mu-L_\tau}$ symmetry is spontaneously broken below the electroweak scale and the Z' acquires the mass,

$$\mathcal{L}_{\mathrm{mass}} = \frac{1}{2}M_{Z'}^2 Z'^\rho Z'_\rho. \qquad (2)$$

We do not introduce the kinetic mixing term between the $U(1)_{L_\mu-L_\tau}$ and the electromagnetic $U(1)_{\mathrm{em}}$ gauge bosons, which are described as [69–71]

$$\mathcal{L}_{\mathrm{mix}} = -\frac{\varepsilon}{2}F_{\rho\sigma}F'^{\rho\sigma}, \qquad (3)$$

where $F_{\rho\sigma}$ and $F'_{\rho\sigma}$ are the field strength of photon and that of Z', i.e., we set $\varepsilon = 0$ at the tree level. The kinetic mixing term can be forbidden by the introduction of the symmetry under the exchange of μ and τ, which is held by the gauge interaction part of the quantum electrodynamics and is softly broken at the lepton mass terms [36,72]. In short, our effective theory that is valid below the scale of the $U(1)_{L_\mu-L_\tau}$ breaking contains only two additional parameters, which are $g_{Z'}$ and $M_{Z'}$. We call this framework the minimal $U(1)_{L_\mu-L_\tau}$ model.

B. Experimental constraints

As mentioned in the introduction, our focus lies on the phenomenology of the gauge boson Z' with a mass around MeV–GeV. Such a light boson interacting with charged leptons, however, is severely constrained by various experiments. In this subsection, we list the constraints relevant to the parameter space we are interested in, which are (i) the neutrino-trident-production process, (ii) neutrino-electron elastic scattering, (iii) muonic Z' search in $e^+e^- \to Z'\mu^+\mu^- \to 2\mu^+2\mu^-$ at the *BABAR* collider, and (iv) Z' search in meson decays. The parameter regions excluded by those experimental results are summarized in Fig. 1. More discussions on the constraints can be found in Refs. [24,26,73,74] and references therein.[3]

---

[2]We refer to an extra $U(1)$ gauge boson as dark photon with a mass below the electroweak scale, which couples to the SM particle content only through the kinetic mixing with photon.

[3]The $L_\mu - L_\tau$ interaction with $g_{Z'} \gtrsim 10^{-5}$ significantly decreases the diffusion rate of neutrinos from supernova. To circumvent the constraint from supernova cooling, the introduction of an invisible particle that promotes the cooling process is required [24].
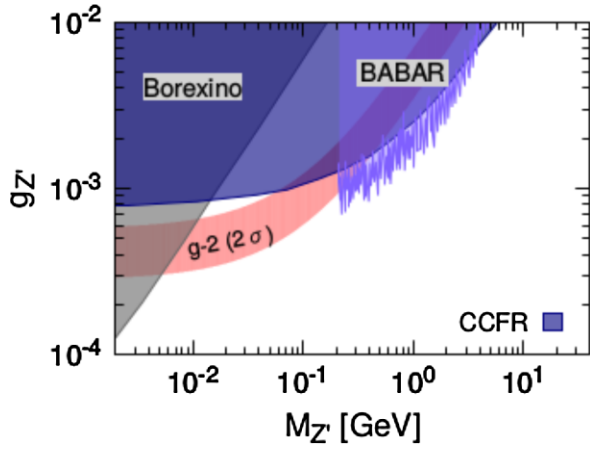
FIG. 1. Summary of the parameter space of the minimal $L_\mu - L_\tau$ model. The regions shaded in blue-gray are excluded by the (i) neutrino-trident-production process [Columbia-Chicago-Fermilab-Rochester (CCFR) experiment], (ii) neutrino-electron elastic scattering (Borexino detector), and (iii) muonic Z' search at the collider (*BABAR*). With the parameters on the red band labeled with "$g-2$," the extra contribution from the one-loop diagram mediated by Z' resolves the discrepancy between the SM prediction and the experimental measurements of muon anomalous magnetic moment within 2σ.

The neutrino-trident-production process, $\nu_\mu N \to \nu_\mu N \mu^+ \mu^-$, where N represents a target nucleus, is a good probe into the light Z', as pointed out in Ref. [75]. Since the cross section measured at the fixed-target neutrino experiments [76,77] was found to be consistent with the SM prediction, the contribution of the Z' must be suppressed so as to agree with the condition

$$\frac{\sigma^{\text{CCFR}}}{\sigma^{\text{SM}}} = 0.82 \pm 0.28. \qquad (4)$$

In Fig. 1, we refer to the 95% C.L. limit based on the result of the CCFR experiment [77]. Prospects of measuring the neutrino-trident-production process at modern neutrino beam experiments were recently discussed in Ref. [78] in the SM, and in Refs. [79,80] in a context of $U(1)_{L_\mu - L_\tau}$ models with the kinetic mixing at the tree level.

The authors of Ref. [81] indicated that the precision measurement of the neutrino-electron elastic scattering can
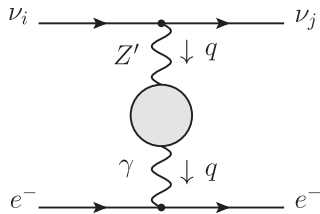

FIG. 2. Diagram of the neutrino-electron scattering process. The one-loop γ-Z' mixing $\varepsilon_{\nu e}$, which is expressed with a shaded blob, is given in Eq. (6).

place a stringent bound on the leptonic force mediated by a light boson. Although the Z' in the minimal $U(1)_{L_\mu - L_\tau}$ model does not couple to electrons at the tree level, the coupling appears through the kinetic mixing induced at the one-loop level, which is calculated to be

$$\Pi(q^2) \equiv \text{[diagram]}$$

$$= \text{[diagram]} + \text{[diagram]}$$

$$= \frac{8eg_{Z'}}{(4\pi)^2} \int_0^1 x(1-x) \ln \frac{m_\tau^2 - x(1-x)q^2}{m_\mu^2 - x(1-x)q^2} \, dx, \qquad (5)$$

where e is the electromagnetic charge, m_ℓ is the mass of the charged lepton ℓ, and q is the momentum carried by γ and Z'. The kinetic mixing parameter ε in Eq. (3) is given as $\varepsilon = \Pi(q^2)$.[4] With the mixing, the Z' comes to contribute to the scattering process illustrated in Fig. 2. The most stringent constraint on the extra contribution to the $\nu - e$ elastic scattering process is provided from the measurement of ^{7}Be solar neutrinos at the Borexino detector [82]. Since the momentum transfer q in the solar neutrino scattering process is much smaller than muon mass, the kinetic mixing parameter $\varepsilon_{\nu e}$ relevant to this scattering process is approximately given as

$$\varepsilon_{\nu e} = \Pi(0) = \frac{8}{3} \frac{eg_{Z'}}{(4\pi)^2} \ln \frac{m_\tau}{m_\mu}. \qquad (6)$$

In Fig. 1, we show the bound from the Borexino experiment, which is converted from the bound to a gauged $U(1)_{B-L}$ model [81].[5] As we see in the next section, the kinetic mixing parameter $\varepsilon_{\text{Belle}}$ that appears in the cross section of our signal process $e^+ e^- \to \gamma Z'$ at the Belle-II experiment is given as

$$\varepsilon_{\text{Belle}} = \Pi(M_{Z'}^2), \qquad (7)$$

which varies by 2 orders of magnitude according to the mass of the Z'. We emphasize that the q dependence of the kinetic mixing makes the phenomenology of the minimal $L_\mu - L_\tau$ model different from that of dark photon models in which the kinetic mixing is given as a constant parameter.

Recently, the *BABAR* collaboration searched for a muonic Z' in the successive processes $e^+ e^- \to \mu^+ \mu^- Z'$

---

[4]In the case where the kinetic mixing term Eq. (3) exists at the tree level, the kinetic mixing parameter ε is understood as $\varepsilon = \varepsilon_{\text{tree}} + \Pi(q^2)$ [79].

[5]The constraints to $\varepsilon_{\nu e}$ are also discussed in Refs. [83,84].

and $Z' \to \mu^+\mu^-$ [85]. Although the signal event suffers from huge electromagnetic backgrounds, it can be discriminated with the help of the invariant mass distribution of the muon pairs in the final state. The constraint given from this process is available only in the parameter region of $M_{Z'} > 2m_\mu$, and we show the 90% C.L., which is provided in Ref. [85], in Fig. 1.

Let us briefly mention the constraints from the Z' search in meson decays. The light Z' can be produced from a muon in the final state in decays of mesons. The search for the Z' in the charged kaon decay process $K^+ \to \mu^+\nu_\mu Z'$ followed by $Z' \to \nu\bar{\nu}$ [86,87] put the bound on the gauge coupling as $g_{Z'} \lesssim 10^{-2}$ in the relevant range of $M_{Z'}$ [72], which is much weaker than the other constraints listed above.

Finally, we make comments on light dark photon searches at the electron and proton beam dumps, in which a pair of the charged leptons (mainly electrons) produced in the decay of the dark photon is hunted as the signal event. Since the Z' in the minimal $L_\mu - L_\tau$ model decays mainly to a pair of neutrinos and the decay branching ratio to an electron pair is negligibly small, the constraints from the beam dump experiments are not applicable to the minimal $L_\mu - L_\tau$ model [26]. The fixed-target muon beam experiment planned by the authors of Ref. [88] will allow us to examine the whole parameter region favored by the muon anomalous magnetic moment in the $L_\mu - L_\tau$ model.

C. Motivation to the light Z'

As is well known, there is a long-standing discrepancy between the experimental measurement [89] and the SM predictions [90–94] of the magnetic moment of muons, which is evaluated as

$$\delta a_\mu = a_\mu^{\rm exp} - a_\mu^{\rm SM} = (28.7 \pm 8.0) \times 10^{-10}, \quad (8)$$

in terms of $a_\mu \equiv (g_\mu - 2)/2$. The new interaction with muons, which is introduced in Eq. (1), provides an extra contribution to a_μ, which is calculated as [8,9][6]

$$a_\mu^{Z'} = \frac{g_{Z'}^2}{8\pi^2} \int_0^1 \frac{2m_\mu^2 x^2(1-x)}{x^2 m_\mu^2 + (1-x)M_{Z'}^2} dx. \quad (9)$$

The parameter region on which the Z' contribution resolves the discrepancy in the muon anomalous magnetic moment at 2σ is indicated with the red band (labeled with $g-2$) in

---

[6]The introduction of the tree-level kinetic mixing $\varepsilon_{\rm tree}$ changes the gauge coupling for muon from $g_{Z'}$ to $e\varepsilon_{\rm tree} + g_{Z'}$. The region excluded by the CCFR and *BABAR* experiments and the region favored by muon $g-2$ shown in Fig. 1 are shifted by this change of the coupling. The cross section of the neutrino-electron scattering process at Borexino is multiplied by $|\varepsilon_{\rm tree} + \varepsilon_{\nu e}|^2/|\varepsilon_{\nu e}|^2$. For more discussion on the parameter region of the $L_\mu - L_\tau$ model with the tree-level kinetic mixing, see Ref. [79].

Fig. 1. After the constraints listed in the previous subsection are taken into consideration, a narrow window of the parameter region,

$$M_{Z'} \simeq [5 \times 10^{-3}, 2 \times 10^{-1}] \text{ GeV}$$
$$g_{Z'} \simeq [3 \times 10^{-4}, 1 \times 10^{-3}], \quad (10)$$

which is favored by the muon $g-2$, is still allowed.

It is interesting to point out that the Z' lies on the parameter region of Eq. (10), resonantly enhancing the scattering of high-energy cosmic neutrinos on the cosmic neutrino background, and the scattering can leave characteristic absorption lines in the cosmic neutrino spectrum observed at the Earth [23]. The IceCube experiment reported a gap in the cosmic neutrino spectrum between 400 TeV and 1 PeV [95],[7] and it was demonstrated in Ref. [26] that the IceCube gap and the discrepancy in the muon anomalous magnetic moment can be simultaneously resolved by the $L_\mu - L_\tau$ force with a set of the parameters in the range of Eq. (10).

III. LIGHT Z' SEARCH AT BELLE-II

We study the feasibility to detect the Z' at the future Belle-II experiment, which is an electron-positron collider with the center-of-mass energy of $\sqrt{s} = 10.58$ GeV designed to achieve the integrated luminosity of 50 ab^{-1} by the middle of the next decade. Although the observation of the muon anomalous magnetic moment favors the parameter region shown in Eq. (10), for the sake of completeness, we broaden our scope of $M_{Z'}$ to [0, 10] GeV, which is the mass range possible to be explored at the Belle-II experiment.

A. Signal: $e^+e^- \to \gamma Z'$, $Z' \to \nu\bar{\nu}$

With the interaction given in Eq. (1), the Z' is produced on its mass shell through the diagram shown in Fig. 3.[8] Depending on its mass, the Z' subsequently decays not only into a pair of neutrinos but also into charged leptons. In this study, we focus on the $Z' \to \nu\bar{\nu}$ decay mode, because the process $e^+e^- \to \gamma + E$, where E denotes missing energies carried by neutrinos, does not suffer from electromagnetic backgrounds, if the final state particles are not missed by the detectors. The Z' is produced through the kinetic mixing, which is given in Eq. (5) as a function of the momentum q carried by Z'. In Fig. 4, we plot the square of the kinetic mixing $|\varepsilon_{\rm Belle}|^2 = |\Pi(q^2 = M_{Z'}^2)|^2$ as a function of E_γ, where E_γ denotes the energy of the final state photon and is related to q^2 as

---

[7]In the four-year IceCube data [96] the gap becomes narrower but still exists.

[8]Note that the one-loop triangle diagrams that prompt $e^+e^- \to \gamma^* \to \gamma Z'$ are canceled with each other due to the Furry's theorem. The same type of cancellation mechanism in the radiative $Z \to \gamma\gamma$ decay is discussed in Ref. [97] and references therein.
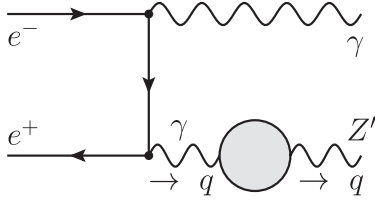
FIG. 3. Diagram of the signal process at the Belle experiment: The Z' production $e^+e^- \rightarrow \gamma Z'$ through the γ-Z' mixing $\varepsilon_{\text{Belle}}$ given in Eq. (7).

$$E_\gamma = \frac{s - q^2}{2\sqrt{s}} \tag{11}$$

in the center-of-mass frame. Here the gauge coupling is taken to be $g_{Z'} = 1.0 \times 10^{-3}$. We also show the value of $\varepsilon_{\nu e}$ given in Eq. (6) as a comparison. The loop-induced kinetic mixing can change by 2 orders of magnitude in the range of $M_{Z'}$, which Belle-II can explore. This feature distinguishes the phenomenology of the $L_\mu - L_\tau$ model from the dark photon models with a constant value of the kinetic mixing. It is clearly recognizable in Fig. 4 that the kinetic mixing $\Pi(q^2)$ is enhanced with a large value of E_γ, which corresponds to a light Z'.

The differential cross section of the signal process $e^+e^- \rightarrow \gamma Z'$ in the center-of-mass frame is found to be [66,98,99]

$$\frac{d\sigma_{\gamma Z'}}{d\cos\theta} = \frac{2\pi\alpha^2 |\Pi(M_{Z'}^2)|^2}{s} \left[1 - \frac{M_{Z'}^2}{s}\right] \frac{1 + \cos^2\theta + \frac{4sM_{Z'}^2}{(s - M_{Z'}^2)^2}}{(1 + \cos\theta)(1 - \cos\theta)}, \tag{12}$$
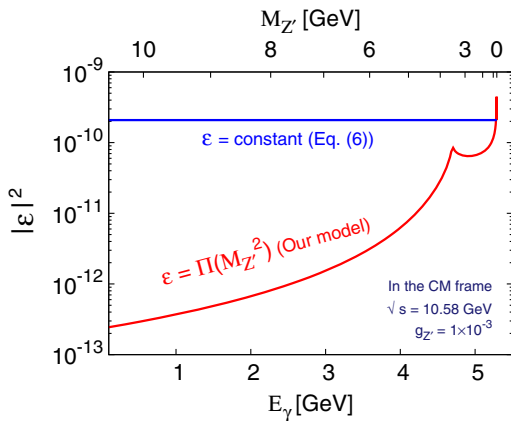

FIG. 4. The γ-Z' mixing Π as a function of the photon energy E_γ (red). The coupling $g_{Z'}$ is taken to be 1×10^{-3}. The upper horizontal axis represents $M_{Z'}$ which is related to E_γ as Eq. (11). We also show $\varepsilon_{\nu e}$ in blue, which is the kinetic mixing parameter appearing in the neutrino-electron elastic scattering and is given in Eq. (6), as a comparison.
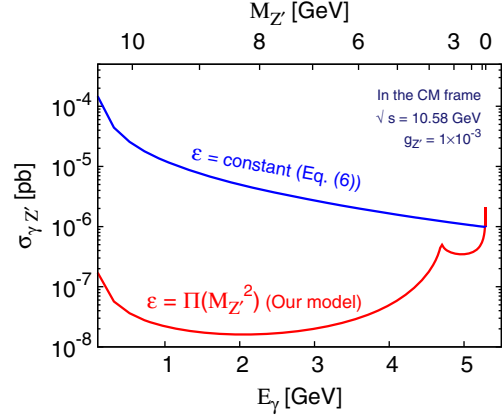

FIG. 5. The cross sections of the Z' production process $e^+e^- \rightarrow \gamma Z'$ as a function of E_γ (lower axis) and $M_{Z'}$ (upper axis). The red and the blue curves correspond to the minimal $U(1)_{L_\mu - L_\tau}$ model and the case with the constant value $\varepsilon_{\nu e}$ for the kinetic mixing, respectively.

where α is the fine structure constant and θ is the angle between the electron beam axis and the photon momentum. The cross section after integrating the angle θ over the range of the coverage of the electromagnetic calorimeters is given as [66]

$$\sigma_{\gamma Z'} = \frac{2\pi\alpha^2 |\Pi(M_{Z'}^2)|^2}{s} \left[1 - \frac{M_{Z'}^2}{s}\right]$$
$$\times \left[\left[1 + \frac{2sM_{Z'}^2}{(s - M_{Z'}^2)^2}\right] \ln\frac{(1 + \cos\theta_{\max})(1 - \cos\theta_{\min})}{(1 - \cos\theta_{\max})(1 + \cos\theta_{\min})}\right.$$
$$\left. - \cos\theta_{\max} + \cos\theta_{\min}\right], \tag{13}$$

where $\cos\theta_{\min} = 0.941$ and $\cos\theta_{\max} = -0.821$ in the center-of-mass frame of the Belle-II experiment. In Fig. 5, the cross section in the minimal $L_\mu - L_\tau$ model is compared to that calculated with the kinetic mixing of the constant value $\varepsilon_{\nu e}$ given in Eq. (6). The cross section of the minimal $L_\mu - L_\tau$ models is enhanced in the high E_γ region due to the q^2 dependence in $\Pi(q^2)$, as illustrated in Fig. 4. The coupling $g_{Z'}$ is taken to be 10^{-3} in the plot, and the cross section is scaled as $g_{Z'}^2$ as seen in the analytic expression of the cross section, Eq. (13).

Since the Z' can decay not only into a pair of neutrinos but also to charged leptons, the rate for the signal process $e^+e^- \rightarrow \gamma Z'$, $Z' \rightarrow \nu\bar{\nu}$ is calculated by multiplying the cross section $\sigma_{\gamma Z'}$ in Eq. (13) by the branching ratio for the $Z' \rightarrow \nu\bar{\nu}$ process, which is given as[9]

---

[9]The Z' can decay also into a pair of electrons through the kinetic mixing. However, the branching ratio is negligibly small.

$$\text{Br}(Z' \to \nu\bar{\nu}) = \begin{cases} 1, & (M_{Z'} < 2m_\mu), \\ \dfrac{\Gamma(Z' \to \nu\bar{\nu})}{\sum_{f=\nu,\mu} \Gamma(Z' \to f\bar{f})}, & (2m_\mu < M_{Z'} < 2m_\tau), \\ \dfrac{\Gamma(Z' \to \nu\bar{\nu})}{\sum_{f=\nu,\mu,\tau} \Gamma(Z' \to f\bar{f})}, & (2m_\tau < M_{Z'}). \end{cases}$$

(14)

The decay rates are calculated to be

$$\Gamma(Z' \to \nu\bar{\nu}) = \frac{g_{Z'}^2}{12\pi} M_{Z'},$$ (15)

$$\Gamma(Z' \to \ell^+\ell^-) = \frac{g_{Z'}^2}{12\pi} M_{Z'} \left[1 + \frac{2m_\ell^2}{M_{Z'}^2}\right] \sqrt{1 - \frac{4m_\ell^2}{M_{Z'}^2}},$$ (16)

where $\ell = \{\mu, \tau\}$.

B. SM background

The signal process $e^+e^- \to \gamma + E$ is also replicated with the SM processes mediated by an off-shell weak boson, which are shown in Fig. 6. They provide the inevitable background event.[10] The diagram shown in the bottom of Fig. 6, in which the final state photon is emitted from the $WW\gamma$ vertex, can be safely eliminated from our evaluation of the background, because the diagram is suppressed by an additional W boson propagator in comparison with the other diagrams. The background processes with muon and tau neutrinos in the final state are led only from the diagram mediated by a Z boson (top of Fig. 6). On the other hand, all the diagrams contribute to the process with a pair of electron neutrinos. The differential cross section of the SM background (BG) is given as

$$\frac{d\sigma_{\text{SM}}}{dE_\gamma} = \frac{\alpha G_F^2}{3\pi^2}(g_L^2 + g_R^2)E_\gamma \left[1 - \frac{2E_\gamma}{\sqrt{s}}\right]$$

$$\times \left[\left[1 - \frac{\sqrt{s}}{E_\gamma} + \frac{s}{2E_\gamma^2}\right] \ln \frac{(1 + \cos\theta_{\max})(1 - \cos\theta_{\min})}{(1 - \cos\theta_{\max})(1 + \cos\theta_{\min})}\right.$$

$$\left. - \cos\theta_{\max} + \cos\theta_{\min}\right]$$

(17)

in the center-of-mass frame, where the couplings are defined as

$$g_L = \begin{cases} -\frac{1}{2} + \sin^2\theta_W & (\text{for } \nu_\mu, \nu_\tau) \\ -\frac{1}{2} + \sin^2\theta_W + 1 & (\text{for } \nu_e) \end{cases}$$

$$g_R = \sin^2\theta_W,$$ (18)

---

[10]We discuss the background events caused by failing to detect the final state particles in Sec. III D. We call the $e^+e^- \to \gamma\nu\bar{\nu}$ process mediated by the weak gauge bosons (shown in Fig. 6) the SM BG.
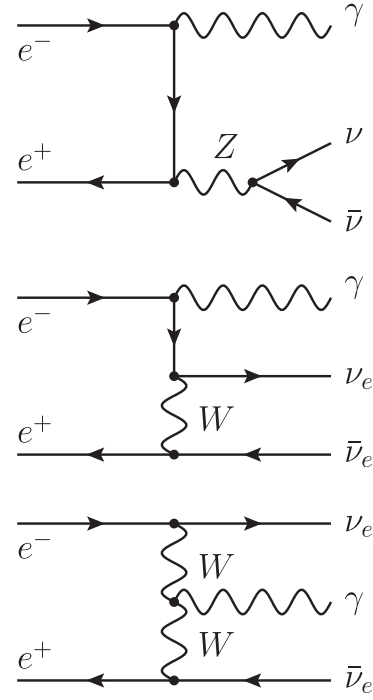

FIG. 6. Diagrams of the SM background. The W boson diagrams produce only electron neutrinos, while the Z boson diagram does all the flavors of neutrinos.

and θ_W is the Weinberg angle. We have checked that Eq. (17) is consistent with the result reported in Ref. [100].

C. Signal significance

The E_γ dependence of the differential cross sections of the signal process $e^+e^- \to \gamma Z' \to \gamma\nu\bar{\nu}$ is compared to that of the SM background in Fig. 7. The cross section Eq. (13) of the signal process is enhanced in the high E_γ region, due to the q^2 dependence of the Π function (cf., Fig. 4), while the SM background is suppressed. Figure 7 shows that the signal with the coupling $g_{Z'} \gtrsim 10^{-3}$ becomes larger than the SM background around the high E_γ end. We emphasize again that the E_γ dependence (equivalent to the $M_{Z'}$ dependence) of the signal is a characteristic feature of the minimal $L_\mu - L_\tau$ model and is different from the dark photon models with a constant kinetic mixing. The signal and the background are compared also in their numbers of event in Fig. 8, where the red histogram shows the $M_{Z'}$ dependence (E_γ dependence) of the signal event N_{sig} and the gray shows the E_γ distribution of the SM background event N_{BG}, respectively. The integrated luminosity $\mathcal{L}$ is assumed to be 50 ab^{-1}. The detector resolution to the photon energy, which is understood also as the width of each energy bin, is taken to be
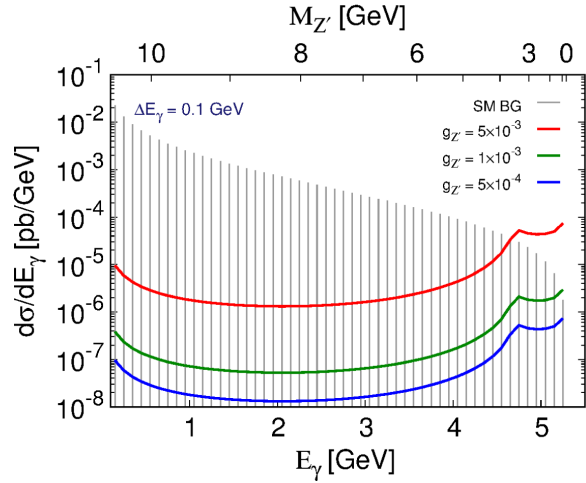
$$\Delta E_\gamma = 0.1 \text{ GeV}$$ (19)

FIG. 7. The differential cross sections as functions of E_γ. The solid curves show the cross sections of the signal process with different values of the couplings $g_{Z'} = \{5 \times 10^{-4}(\text{blue}), 1 \times 10^{-3}(\text{green}), 5 \times 10^{-3}(\text{red})\}$. The cross sections are calculated with the value of $M_{Z'}$ indicated with the top horizontal axis. The E_γ dependence of the SM background cross section is shown as the region shaded with gray vertical stripes.

[101]. Here, we assume that the energy resolution in the center-of-mass frame is the same as the one in the laboratory frame. The error bars indicate the range of the 3σ statistical error estimated with the square root of the number of the background event, $\sqrt{N_{\mathrm{BG}}}$. The number of the signal event with the coupling $g_{Z'} = 10^{-3}$ exceeds the SM background more than 3σ in the highest energy bin, which corresponds to the Z' with $M_{Z'} \lesssim 1$ GeV. From this result, we can expect that the Belle-II experiment will be sensitive to the light Z' ($M_{Z'} \lesssim 1$ GeV) with the coupling $g_{Z'} \gtrsim 10^{-3}$.
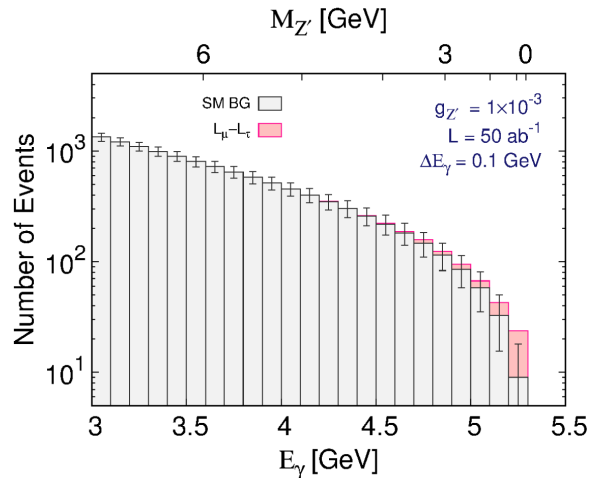
In order to illustrate the parameter region on which the Belle-II experiment can detect the Z' through the signal process $e^+e^- \rightarrow \gamma + E$, we define the signal significance $\mathcal{S}$ as

$$\mathcal{S} \equiv \frac{N_{\mathrm{sig}}(g_{Z'}, M_{Z'})}{\sqrt{N_{\mathrm{BG}}}} \quad (20)$$

and adopt $\mathcal{S} > 3$ for the criterion of the signal detection, i.e., we expect that Belle-II will be sensitive to the parameter sets $(g_{Z'}, M_{Z'})$ that satisfy the criterion. In Fig. 9, we draw the boundaries of the parameter regions that will be examined by the Belle-II experiment with three different integrated luminosities $\mathcal{L} = \{10, 50, 100\}$ ab^{-1}. The signal significance $\mathcal{S}$ exceeds 3 on the regions of the upper side of each curve. The regions shaded in gray are excluded by the experimental constraints listed in Sec. II B (CCFR, Borexino, and *BABAR*). The red band indicates the parameters favored by muon $g - 2$ within 2σ. We also show in yellow the parameter region favored by the discrepancy in a_μ with the value of

$$\delta a_\mu = (4.8 \pm 1.6) \times 10^{-10}, \quad (21)$$

where we expect that the error in a_μ will be reduced by a factor of 5 in future experiments [102,103] and assume that the discrepancy will be kept at 3σ. It is shown that the Belle-II experiment with the full integrated luminosity is expected to be sensitive to the parameter region with $M_{Z'} \lesssim 1$ GeV and $g_{Z'} \gtrsim 8 \times 10^{-4}$. The sensitivity becomes improved with a higher luminosity such as $\mathcal{L} = 100$ ab^{-1}, because the significance is proportional to $\sqrt{\mathcal{L}}$. We examine the possible improvements in the sensitivity with the change of the energy resolution ΔE_γ and the

FIG. 8. E_γ distribution of the event numbers. The red histogram shows the number of the signal events N_{sig} calculated with the coupling $g_{Z'} = 10^{-3}$ and the mass $M_{Z'}$ indicated with the upper horizontal axis, while the gray shows the SM background events N_{BG}. The integrated luminosity is assumed to be 50 ab^{-1}. The error bars indicate the range of the 3σ statistical error.
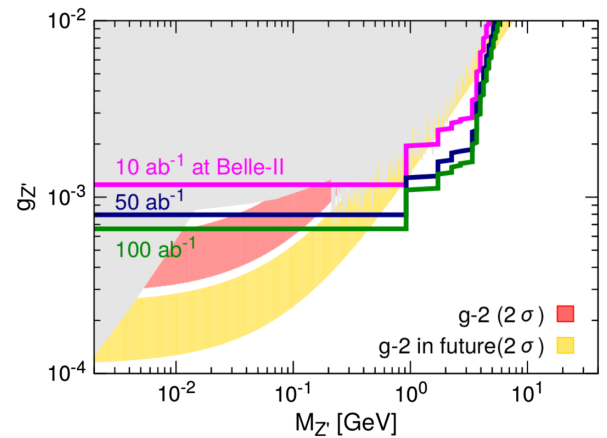

FIG. 9. Parameter regions with the signal significance $\mathcal{S}$ larger than 3. The integrated luminosity is taken to be 10 (magenta), 50 (blue), and 100 (green) ab^{-1}. The experimental constraints summarized in Fig. 1 are shown in gray. The red and yellow bands indicate the parameter regions favored by the current [Eq. (8)] and the future [Eq. (21)] muon $g - 2$ measurements.
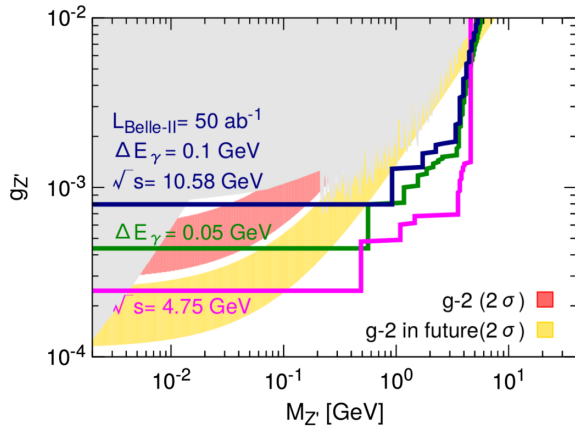
FIG. 10. The same plot as Fig. 9 with $\Delta E_\gamma = 0.05$ GeV (green) and $\sqrt{s} = 4.75$ GeV (magenta). These correspond to the setup given in Eq. (22).

center-of-mass energy $\sqrt{s}$. We compare the sensitivity reaches estimated with the following two sets of parameters,

$$(\Delta E_\gamma, \sqrt{s}) = \begin{cases} (0.05 [\text{GeV}], 10.58 [\text{GeV}]), & (\text{green}), \\ (0.1 [\text{GeV}], 4.75 [\text{GeV}]), & (\text{magenta}), \end{cases} \tag{22}$$

in Fig. 10. The event number of the signal process is inversely proportional to s [cf., Eq. (13)],

$$N_{\text{sig}} \propto 1/s, \tag{23}$$

and hence it is enhanced with a lower value of the center-of-mass energy, while the SM background depends on $\sqrt{s}$ and ΔE_γ as [cf., Eq. (17)]

$$N_{\text{BG}} \propto \sqrt{s} \Delta E_\gamma, \tag{24}$$

which is reduced with a lower $\sqrt{s}$ and a smaller ΔE_γ. Figure 10 shows that the region favored by the current measurement of muon $g-2$ at 2σ is completely covered by the sensitivity reach of the Belle-II experiment with the center-of-mass energy $\sqrt{s} = 4.75$ GeV and $\mathcal{L} = 50$ ab^{-1}.

D. Another possible background: $e^+ e^- \to \gamma + undetected$

We have estimated the number of the inevitable background event mediated by the weak interaction and discussed the signal significance and the sensitivity reach in the previous subsections. However, because of the limitation in detector coverage and detection efficiency, it is possible that the electromagnetic processes $e^+ e^- \to \gamma + X$ with undetected final states X come into backgrounds. The undetected state X can be $n\gamma$ ($n \geq 1$), $e^+ e^-$, etc. It is pointed out in Refs. [65,67,68] that the process with $X = \gamma$

can be a serious background in the detection of light Z', because the signal photon shows the same kinematics as the photons in the background event up to the order of $M_{Z'}^2/s$. Since the undetection rate of the photon at the Belle-II experiment strongly depends on its detector properties, an estimation of the rate requires a dedicated detector simulation. In this study, we expect that the detection efficiency for photons with energies of $\sqrt{s}/2$ is high enough to reconstruct perfectly the back-to-back two photon events, $e^+ e^- \to \gamma\gamma$. We carry out a numerical simulation, which is specialized to the experimental setup of Belle II, to optimize the kinematical cuts so as to maximize the signal significance, in a forthcoming paper.

IV. CONCLUSIONS AND DISCUSSION

We have discussed the sensitivity of the Belle-II experiment to the light gauge boson Z' in the minimal gauged $U(1)_{L_\mu - L_\tau}$ model. With the new gauge interaction, the Z' is produced through the kinetic mixing between the photon and Z', which is absent at the tree level but is induced radiatively. We have focused on $e^+ e^- \to \gamma Z' \to \gamma \nu \bar{\nu}$ as the signal process, because it does not suffer from a huge number of electromagnetic background events, as long as the undetection rate of high-energy photons is sufficiently suppressed. Differing from the search for a dark photon with a constant kinetic mixing (e.g., Ref. [67]), the signal event in the $U(1)_{L_\mu - L_\tau}$ model is strongly enhanced with a small $M_{Z'}$, with which the inconsistency in the muon anomalous magnetic moment and the gap in the IceCube spectrum can be simultaneously explained [23]. The cross section of the signal event reaches $\mathcal{O}(1)$ ab with the parameters $g_{Z'} = 10^{-3}$ and $M_{Z'} < 1$ GeV, i.e., $\mathcal{O}(10)$ events are expected at the Belle-II experiment with the design luminosity. We have estimated the number of background events and calculated the signal significance to illustrate the parameter region to which the Belle-II experiment will be sensitive. The SM background events are distributed more in the lower energy regions of the final state photon. We have shown that the signal events with a high-energy photon, which corresponds to a low $M_{Z'}$, can be discriminated from the background events. We have found that the Belle-II experiment with the design luminosity can examine a part of the parameter region that evades the current experimental constraints and, at the same time, is favored by the observation of the muon anomalous magnetic moment. We have shown that the further improvement in sensitivity is possible with an increase of the luminosity, an adjustment of the center-of-mass energy, and the upgrading of the energy resolution of the calorimeter.

As a concluding remark, we emphasize that our analysis can be easily generalized to any models with a light Z' that has an invisible decay channel and loop-induced kinetic mixing.

ACKNOWLEDGMENTS

[1] G. Aad *et al.* (ATLAS Collaboration), Phys. Lett. B **716**, 1 (2012).

[2] S. Chatrchyan *et al.* (CMS Collaboration), Phys. Lett. B **716**, 30 (2012).

[3] Y. Fukuda *et al.* (Super-Kamiokande Collaboration), Phys. Rev. Lett. **81**, 1562 (1998).

[4] Q. R. Ahmad *et al.* (SNO Collaboration), Phys. Rev. Lett. **87**, 071301 (2001).

[5] G. Bertone, D. Hooper, and J. Silk, Phys. Rep. **405**, 279 (2005).

[6] S. Perlmutter *et al.* (Supernova Cosmology Project Collaboration), Astrophys. J. **517**, 565 (1999).

[7] A. G. Riess *et al.* (Supernova Search Team Collaboration), Astron. J. **116**, 1009 (1998).

[8] S. N. Gninenko and N. V. Krasnikov, Phys. Lett. B **513**, 119 (2001).

[9] S. Baek, N. G. Deshpande, X. G. He, and P. Ko, Phys. Rev. D **64**, 055006 (2001).

[10] A. J. Krasznahorkay *et al.*, Phys. Rev. Lett. **116**, 042501 (2016).

[11] J. L. Feng, B. Fornal, I. Galon, S. Gardner, J. Smolinsky, T. M. P. Tait, and P. Tanedo, Phys. Rev. Lett. **117**, 071803 (2016).

[12] P.-H. Gu and X.-G. He, arXiv:1606.05171.

[13] J. L. Feng, B. Fornal, I. Galon, S. Gardner, J. Smolinsky, T. M. P. Tait, and P. Tanedo, arXiv:1608.03591.

[14] T. Kitahara and Y. Yamamoto, Phys. Rev. D **95**, 015008 (2017).

[15] O. Seto and T. Shimomura, arXiv:1610.08112.

[16] S. Hannestad, R. S. Hansen, and T. Tram, Phys. Rev. Lett. **112**, 031802 (2014).

[17] B. Dasgupta and J. Kopp, Phys. Rev. Lett. **112**, 031803 (2014).

[18] Z. Tabrizi and O. L. G. Peres, Phys. Rev. D **93**, 053003 (2016).

[19] K. Ioka and K. Murase, Prog. Theor. Exp. Phys. **2014**, 061E01 (2014).

[20] K. C. Y. Ng and J. F. Beacom, Phys. Rev. D **90**, 065035 (2014).

[21] M. Ibe and K. Kaneta, Phys. Rev. D **90**, 053011 (2014).

[22] K. Blum, A. Hook, and K. Murase, arXiv:1408.3799.

[23] T. Araki, F. Kaneko, Y. Konishi, T. Ota, J. Sato, and T. Shimomura, Phys. Rev. D **91**, 037301 (2015).

[24] A. Kamada and H.-B. Yu, Phys. Rev. D **92**, 113004 (2015).

[25] A. DiFranzo and D. Hooper, Phys. Rev. D **92**, 095007 (2015).

[26] T. Araki, F. Kaneko, T. Ota, J. Sato, and T. Shimomura, Phys. Rev. D **93**, 013014 (2016).

[27] I. M. Shoemaker and K. Murase, Phys. Rev. D **93**, 085004 (2016).

[28] V. Barger, C.-W. Chiang, W.-Y. Keung, and D. Marfatia, Phys. Rev. Lett. **106**, 153001 (2011).

[29] D. Tucker-Smith and I. Yavin, Phys. Rev. D **83**, 101702 (2011).

[30] S. G. Karshenboim, D. McKeen, and M. Pospelov, Phys. Rev. D **90**, 073004 (2014); **90**, 079905 (2014).

[31] C. E. Carlson and M. Freid, Phys. Rev. D **92**, 095024 (2015).

[32] N. Arkani-Hamed, D. P. Finkbeiner, T. R. Slatyer, and N. Weiner, Phys. Rev. D **79**, 015014 (2009).

[33] J. L. Feng, M. Kaplinghat, and H.-B. Yu, Phys. Rev. D **82**, 083525 (2010).

[34] R. Foot, Mod. Phys. Lett. A **06**, 527 (1991).

[35] X. He, G. C. Joshi, H. Lew, and R. Volkas, Phys. Rev. D **43**, R22 (1991).

[36] R. Foot, X. G. He, H. Lew, and R. R. Volkas, Phys. Rev. D **50**, 4571 (1994).

[37] S. Baek and P. Ko, J. Cosmol. Astropart. Phys. 10 (2009) 011.

[38] S. Baek, Phys. Lett. B **756**, 1 (2016).

[39] S. Patra, S. Rao, N. Sahoo, and N. Sahu, arXiv: 1607.04046.

[40] A. Biswas, S. Choubey, and S. Khan, arXiv:1612.03067.

[41] W. Altmannshofer, S. Gori, M. Pospelov, and I. Yavin, Phys. Rev. D **89**, 095033 (2014).

[42] A. Crivellin, G. DAmbrosio, and J. Heeck, Phys. Rev. Lett. **114**, 151801 (2015).

[43] W. Altmannshofer, S. Gori, S. Profumo, and F. S. Queiroz, J. High Energy Phys. 12 (2016) 106.

[44] J. Heeck, M. Holthausen, W. Rodejohann, and Y. Shimizu, Nucl. Phys. **B896**, 281 (2015).

[45] S. Choubey and W. Rodejohann, Eur. Phys. J. C **40**, 259 (2005).

[46] T. Ota and W. Rodejohann, Phys. Lett. B **639**, 322 (2006).

[47] J. Heeck and W. Rodejohann, J. Phys. G **38**, 085005 (2011).

[48] J. Heeck and W. Rodejohann, Phys. Rev. D **84**, 075007 (2011).

[49] A. Biswas, S. Choubey, and S. Khan, J. High Energy Phys. 09 (2016) 147.

[50] P. Fayet, Nucl. Phys. **B347**, 743 (1990).

[51] P. Fayet, Phys. Rev. D **74**, 054034 (2006).

[52] P. Fayet, Phys. Rev. D **75**, 115017 (2007).

[53] P. Fayet, Phys. Lett. B **675**, 267 (2009).

[54] M. Pospelov, Phys. Rev. D **80**, 095002 (2009).

[55] H. Davoudiasl, H.-S. Lee, and W. J. Marciano, Phys. Rev. D **89**, 095006 (2014).

[56] K. Petraki, L. Pearce, and A. Kusenko, J. Cosmol. Astropart. Phys. 07 (2014) 039.

[57] R. Foot and S. Vagnozzi, Phys. Rev. D **91**, 023512 (2015).

[58] J. Kile, A. Kobach, and A. Soni, Phys. Lett. B **744**, 330 (2015).

[59] Y. Farzan and I. M. Shoemaker, J. High Energy Phys. 07 (2016) 033.

[60] H.-S. Lee and S. Yun, Phys. Rev. D **93**, 115028 (2016).

[61] W. Altmannshofer, C.-Y. Chen, P. S. Bhupal Dev, and A. Soni, Phys. Lett. B **762**, 389 (2016).

[62] Y. Farzan and J. Heeck, Phys. Rev. D **94**, 053010 (2016).

[63] P. Ko and Y. Tang, Phys. Lett. B **762**, 462 (2016).

[64] P. Fayet, Eur. Phys. J. C **77**, 53 (2017).

[65] B. Aubert et al. (BABAR), in Proceedings, 34th International Conference on High Energy Physics (ICHEP 2008): Philadelphia, Pennsylvania, July 30–August 5, 2008.

[66] R. Essig, P. Schuster, and N. Toro, Phys. Rev. D **80**, 015003 (2009).

[67] R. Essig, J. Mardon, M. Papucci, T. Volansky, and Y.-M. Zhong, J. High Energy Phys. 11 (2013) 167.

[68] J. P. Lees et al. (BABAR Collaboration), arXiv:1702.03327.

[69] B. Holdom, Phys. Lett. **166B**, 196 (1986).

[70] R. Foot and X.-G. He, Phys. Lett. B **267**, 509 (1991).

[71] K. S. Babu, C. F. Kolda, and J. March-Russell, Phys. Rev. D **57**, 6788 (1998).

[72] M. Ibe, W. Nakano, and M. Suzuki, arXiv:1611.08460.

[73] R. Laha, B. Dasgupta, and J. F. Beacom, Phys. Rev. D **89**, 093025 (2014).

[74] K. Harigaya, T. Igari, M. M. Nojiri, M. Takeuchi, and K. Tobe, J. High Energy Phys. 03 (2014) 105.

[75] W. Altmannshofer, S. Gori, M. Pospelov, and I. Yavin, Phys. Rev. Lett. **113**, 091801 (2014).

[76] D. Geiregat et al. (CHARM-II Collaboration), Phys. Lett. B **245**, 271 (1990).

[77] S. Mishra et al. (CCFR Collaboration), Phys. Rev. Lett. **66**, 3117 (1991).

[78] G. Magill and R. Plestid, arXiv:1612.05642.

[79] Y. Kaneta and T. Shimomura, arXiv:1701.00156.

[80] S.-F. Ge, M. Lindner, and W. Rodejohann, arXiv:1702.02617.

[81] R. Harnik, J. Kopp, and P. A. N. Machado, J. Cosmol. Astropart. Phys. 07 (2012) 026.

[82] G. Bellini et al., Phys. Rev. Lett. **107**, 141302 (2011).

[83] S. K. Agarwalla, F. Lombardi, and T. Takeuchi, J. High Energy Phys. 12 (2012) 079.

[84] S. Bilmis, I. Turan, T. M. Aliev, M. Deniz, L. Singh, and H. T. Wong, Phys. Rev. D **92**, 033009 (2015).

[85] J. P. Lees et al. (BABAR Collaboration), Phys. Rev. D **94**, 011102 (2016).

[86] A. V. Artamonov et al. (BNL-E949 Collaboration), Phys. Rev. D **79**, 092004 (2009).

[87] A. V. Artamonov et al. (BNL-E949 Collaboration), Phys. Rev. D **91**, 052001 (2015); **91**, 059903(E) (2015).

[88] S. N. Gninenko, N. V. Krasnikov, and V. A. Matveev, Phys. Rev. D **91**, 095015 (2015).

[89] G. Bennett et al. (Muon g-2 Collaboration), Phys. Rev. D **73**, 072003 (2006).

[90] K. Melnikov and A. Vainshtein, Phys. Rev. D **70**, 113006 (2004).

[91] M. Davier, A. Hoecker, B. Malaescu, and Z. Zhang, Eur. Phys. J. C **71**, 1515 (2011); M. Davier, A. Hoecker, B. Malaescu, and Z. Zhang, Eur. Phys. J. C **72**, 1874(E) (2012).

[92] K. Hagiwara, R. Liao, A. D. Martin, D. Nomura, and T. Teubner, J. Phys. G **38**, 085003 (2011).

[93] T. Aoyama, M. Hayakawa, T. Kinoshita, and M. Nio, Phys. Rev. Lett. **109**, 111808 (2012).

[94] A. Kurz, T. Liu, P. Marquard, and M. Steinhauser, Phys. Lett. B **734**, 144 (2014).

[95] M. G. Aartsen et al. (IceCube Collaboration), Phys. Rev. Lett. **113**, 101101 (2014).

[96] M. G. Aartsen et al. (IceCube Collaboration) in Proceedings, 34th International Cosmic Ray Conference (ICRC 2015): The Hague, The Netherlands, July 30–August 6, 2015.

[97] E. V. Zhemchugov, Phys. At. Nucl. **77**, 1390 (2014).

[98] C. Boehm and P. Fayet, Nucl. Phys. **B683**, 219 (2004).

[99] N. Borodatchenkova, D. Choudhury, and M. Drees, Phys. Rev. Lett. **96**, 141802 (2006).

[100] E. Ma and J. Okada, Phys. Rev. Lett. **41**, 287 (1978); **41**, 1759(E) (1978).

[101] T. Abe et al. (Belle-II Collaboration), arXiv:1011.0352.

[102] J. Grange et al. (Muon g-2 Collaboration), arXiv:1501.06858.

[103] M. Aoki et al. (KEK E34 Collaboration), http://g-2.kek.jp/portal/documents.html, 2015.